Check for updates

Energy management considering multiple power markets and microgrid storage

Mengxuan Yan[1,2], Zhanlian Li[1], Chun Sing Lai[1,3]*, Zhuoli Zhao[1], Ahmed F. Zobaa[3], Loi Lei Lai[1] and Zebing Shi[4]

[1]School of Automation, Guangdong University of Technology, Guangzhou, China, [2]Jiangmen Power Supply Bureau of Guangdong Power Grid Co Ltd., Jiangmen, China, [3]Department of Electronic and Electrical Engineering, Brunel University London, Uxbridge, United Kingdom, [4]China Southern Power Grid Co. Ltd., Guangzhou, China

The operational cost of a microgrid is significantly influenced by the response of storage systems and the complexities of the power market's tariff structures. This paper addresses the challenges arising from the coexistence of new market entries and traditional tariffs, which contribute to a complex market environment. To tackle this issue, the paper establishes a microgrid market environment encompassing four types of tariffs. By modeling the response of electric storage and cold storage in a microgrid, the study formulates a non-linear mixed-integer optimization problem. Numerical studies are then conducted to verify the model and analyze market performance. The results reveal a trade-off in behavior among different market entries when optimizing the total cost of microgrid operation. These findings shed light on the complexities and trade-offs involved in microgrid operational cost optimization within a diverse market environment, offering valuable insights for market participants.

KEYWORDS

coordinated operation, natural gas network, electrical network, credit rank indicator, microgrid

1 Introduction

Power market deregulation brings competitive trading to generation and consumer areas. Multiple market participants from both sides are allowed to submit their bids and are matched by market operators (Tabar et al., 2019; Tian et al., 2023). Unlike a regulated power market, deregulated trading may contain more uncertainties, which leads to a higher risk. Thus, a deregulated power market may contain multiple sub-markets to hedge the risk of uncertainties, such as a wholesale market, spot market, capacity market, and several ancillary markets in PJM (Rabiee et al., 2016; Fan et al., 2022; MansourLakouraj et al., 2022). In general, power market deregulation will improve the entire efficiency of power system operation and management. It can also promote the latest technologies by constructing specified market structures (He et al., 2016; Chen et al., 2021; Zhang et al., 2023).

Energy management in a microgrid has become an important issue in recent studies. Nowadays, energy management strategies are growing rapidly (Zhao et al., 2023). In this paper, a new energy management strategy has been proposed for a hybrid microgrid, including demand response and the internal power market (Al-Awami et al., 2017). In this regard, a configuration of multiple markets is considered in the proposed method, and interactions between the consumers, microgrid, and incentive strategies are included in the

presented planning (Garcia-Torres et al., 2020; Huang et al., 2020). Due to the presence of various types of consumers, such as critical and normal loads, different power tariffs and contracts are utilized in energy management. Energy storage is an attractive area for academic and industrial researchers. It presents significant capabilities in power system efficiency enhancement, renewable energy integration, and demand response (Zhao et al., 2012; Zhao and Ding, 2017; Lin et al., 2019; Wang et al., 2021). It also improves the stability and reliability of the power grid (Zhao et al., 2017). Energy storage is also popular in microgrid operations. In a microgrid, energy storage helps in reducing risks due to the intermittence of renewable energy (Kwon et al., 2016; Olabi, 2017; Khaloie et al., 2021; Li et al., 2021). A coalitional game model for the trading of a biomass power plant (BPP) integrated with PV and wind farms was proposed (Khalilpour and Vassallo, 2016; Zhang et al., 2017a; Lai and McCulloch, 2017). It reported the need to have a different method to calculate the energy generation cost due to the installation of energy storage in solar energy production (Lai and McCulloch, 2016). The sizing requirements of solar PV and storage systems need to be considered in relation to biogas power plants. Solar irradiance could be affected by fluctuations introduced by passing clouds. The analysis of these fluctuations with regard to solar energy production could be focused by studying the instantaneous clearness index.

Demand response is another application of energy storage in minimizing the difference between peak and valley loads (Hakimi and Moghaddas-Tafreshi, 2014a; Zhang et al., 2017b; Lai et al., 2017c). Lai et al. (2017a) and Lai et al. (2017b) reported the future of energy storage applications with a focus on large-scale solar energy penetration. Chen et al. (2013), Amrollahi and Bathaee (2017) and Liu et al. (2018) reported the impact of energy storage degradation costs. Vehicle to Grid (V2G) technology is also a popular area for energy storage utilization. As an energy storage unit, batteries of electric vehicles (EVs) participate in microgrid peak shaving and frequency modulation (Lai and McCulloch, 2016; Lai et al., 2017a; Lai et al., 2017b). Gough et al. (2017) proposed an energy storage system (ESS) to minimize the total operation cost of the microgrid. The proposed model constructs an ESS with both electrical and cooling storage to simulate performance in the energy market (Hakimi and Moghaddas-Tafreshi, 2014b; Zidan et al., 2015; Valinejad et al., 2020; Rostamnezh et al., 2022).

By reviewing the aforementioned materials, at least three areas for improvement have been identified:

1. Decision makers in the microgrid and energy storage sectors face the challenge of choosing from multiple markets while aiming to minimize operating costs. In order to navigate these complex market entries, it is crucial to consider both market opportunities and tariff capability distribution. By assessing the available market opportunities and understanding the distribution of tariffs, decision makers can optimize their strategies for achieving minimum operating costs.
2. Microgrids in China have multiple market entries, including markets created by recent evolution and existing traditional tariffs. New regulations may lead to different storage responses in microgrids.

3. In many research works (Jiang et al., 2022), the cold generation in a cooling system is linearly modeled with boundary constraints and a steady coefficient of performance (COP). Chillers of cold generations operate non-linearly with non-steady-state COP.

The main contributions of this work are as follows:

- This paper presents a complex market environment for the microgrid with up to four different parallel tariffs. This environment represents a transition period in the initial stage of change.
- Both electricity and thermal network operations for storage response analysis have been considered. A dynamic COP from historical operational data was developed. Furthermore, this paper considers the pumping power switching mechanism in a cooling system with logical variables. These logical variables create the optimization of a cooling network and formulate a non-linear mixed-integer programming problem.
- Practically, different tariffs may not prevent the same economic values from generating multiple minimum points for optimization. In this case, not all local optimal solutions have a high industrial potential for change in behavior. This paper introduces a new regulation term in the objective function for less behavioral variation to increase the industrial implementation potential of the model.
- Numerical investigation is implemented for model verification and further analysis. Three different studies are selected for impact analysis from different market tariffs. The results show that trading-off occurs in response to storage toward different market entries.

This paper is organized as follows: multiple microgrid market entries are introduced in Section 2. Relevant storage response modeling and simulation construction are shown in Section 3. Section 4 gives a numerical study for storage response analysis. The conclusion is provided in Section 5.

2 Multiple market entries for a microgrid

2.1 Dynamic daily electricity price

In the retail section of catalog price, time-of-use (TOU) is implemented.

In the latest power market evolution, trading of contracts for differences (CFDs) is introduced. For price difference (PD) trading, bilateral negotiation (BN) and monthly bidding (MB) are constructed. A BN market is a yearly market that allows consumers and power plants to deploy transactions. Their trading willingness will be submitted to the power dispatch center for feasibility verification. The submission of BN takes place once a year. In an MB market, power consumption bids and generation bids are received. The market operators match bids with the consideration of dispatch feasibility. The submission of MB takes place once a month. For a dynamic daily price scheme, such as TOU, PD is compensated to give prices for each hour so that the shape of TOU remains the same to fulfill the requirements in catalog price (CP). Eq. 1 gives the power consumption cost with CP based on PD.

$$\begin{cases} C_{TOU} = \sum_{t=1}^{T} S \cdot P_{netload}(t) \cdot TL \cdot A_{TOU}^E(t), \\ P_{netload}(t) = P_{load} - P_{ES}^{dis} - P_{PV}, \\ A_{TOU,i}^E(t) \overset{'}{=} A_{TOU,i}^E(t) - A_i^E, i = 1, 2, ..., 5, \end{cases} \quad (1)$$

$$S = \begin{cases} 1, P_{load} > P_{PV}, \\ 0, P_{load} \leq P_{PV}, \end{cases} \quad (2)$$

where C_{TOU} represents the cost of power consumption from the daily dynamic electricity price. P_{load} represents the total power time series vector. P_{PV} represents the total power generation vector. TL is a time step, with a step length of 15 min$^{'}$. $A_{TOU,i}^E(t)$ represents the dynamic daily electricity price vector. A_i^E is the bid-matched price difference. The dynamic daily electricity price in China does not cover the bi-directional power flow. When electricity storage wins the bids in MRGPAS, the charging of electricity storage is covered and will not be charged again in dynamic daily electricity price calculation.

2.2 Capacity-based charging (CBC)

Two-part tariff is a pricing scheme for electricity in China. The first part is the daily electricity price mentioned previously. The second part is the basic price or capacity price, which is charged on CNY/kVA or CNY/kW. In Hong Kong, basic price is also called demand charge. The basic price is charged on the monthly maximum consumer injecting power or the maximum capacity of a consumer-based local transformer. In recent years, there has been an evolution in the power market, with the advancement of new technologies and the implementation of new policies aimed at promoting sustainable energy practices. Eq. 3 gives the cost generated from the basic price.

$$C_{capacity} = \max(S \cdot P_{netload} \cdot A_{chr}^E), \quad (3)$$

where $C_{capacity}$ represents the cost generated from the basic price. A_{chr}^E represents the price of capacity-based charging. The function max( ) receives a vector and returns the maximum value from the inputted vector.

2.3 Macro-renewable generation promoting ancillary services (MRGPAS)

The market construction of ancillary services is one of the main tasks of power market deregulation in China. Unlike traditional ancillary services, this ancillary service market is specially designed for power peak shaving in supporting renewable generation. Energy storage inside consumers can trade mainly with wind power plants or solar power plants on the ancillary service trading platform to reduce the amount of abandoned wind/solar generation (Xu et al., 2012).

Wind/solar generation abandonment is an obvious phenomenon that occurs in the preliminary stage of renewable power development. For example, in wind generation, when the load decreases, the generation capability of thermal power plants is reduced with higher priority under power dispatch regulation in China. The reason for this is that the marginal cost of generation in wind farms is zero, and the government promotes the development

of renewable energy. However, thermal units have lower operational bounds. The generation of thermal plants cannot be reduced over this bound for the start and stop of large cost of units. When a lower bound of thermal units is reached, wind generation abandonment occurs. As load reduction usually occurs at nighttime, wind generation abandonment and the trading chances of MRGPAS for electricity storage usually occur at night. In some MRGPAS markets, electricity storages of consumers' microgrids can only trade with wind/solar power plants (Kumar and Palanisamy, 2020).

In a MRGPAS market, owners of electricity storages and power plants should submit their bids to the trading platform. The information includes the compensation price, trading time and time length, charging power, and 15-min time step load curves. The market operator matches bids from electricity storages and wind power plants with the consideration of grid operational constraints. When bids are matched, the storage should be charged with a certain compensation price. MRGPAS markets in some provinces have upper and lower limits for the compensation price. The upper and lower limits of the compensation price in a typical market in China are 0.2 CNY/kWh and 0.1 CNY/kWh, respectively. Eq. 4 gives the cost generated from MRGPAS.

$$C_{anci} = (-1) \cdot \sum_{t=1}^{96} [H(t) \cdot P_{anci}(t) \cdot TL \cdot A_{anci}^E(t)], \quad (4)$$

$$H(t) = \begin{cases} 0, \text{fail to bid} \\ 1, \text{successful to bid} \end{cases}, \quad (5)$$

where C_{anci} represents the cost generated from MRGPAS. A_{anci}^E represents the matched compensation price in MRGPAS. H represents the microgrid chances of MRGPAS participation in a day. P_{anci} represents the charging range of electricity storage in bids of macro-renewable-generation promoting ancillary services (MRGPAS), which will be described later. The element H(t) in Eq. 5 is a logical variable, with 0 and 1 representing the microgrid's failed and successful bids at the time step, respectively.

2.4 Distributed solar generation feedback tariff

To enhance clean power generation and support relevant local industries, the Chinese government provides its first bi-directional tariff for microgrids on distributed PV generation. Consumers with distributed PV have two sub-tariff selections. The first sub-tariff is named full feed-in tariff (FFI). The PV operator is required to feed-in all its capacity to the power grid with specified installed protection and meters. The connection point of PV is not inside consumers in FFI, and consumer behavior is fully decoupled with PV generation variation. Therefore, FFI does not influence operation of the microgrid. The second sub-tariff is named surplus feed-in tariff (SFI). In SFI, consumers will consume PV generation as a priority. If surplus PV generation exists, this surplus capacity can be fed into the grid. In SFI, consumer behavior and PV time series generation will influence each other. Consumers with distributed PV can select either FFI or SFI. This paper mainly focuses on SFI modeling for its high integration capability with storage response. Eq. 5 gives the cost generated from SFI.

$$PV\_cha = Comp + Ben. \tag{6}$$

In Eq. 6, *PV_cha* represents the cost generated from the PV tariff. The cost generated from SFI is constructed in two parts. The first part, *Comp*, is from the compensation of governmental policy (Chen et al., 2013). The Chinese government offers compensation for all power generated under the full feed-in tariff (FFI) and surplus feed-in tariff (SFI). The second part, *Ben*, is the benefit from the surplus capacity feeding into the grid at the consumer side for SFI only. Eq. 7 calculates *Comp* and *Ben*, where negative 1 represents customer benefit.

$$\begin{cases} \text{Comp} = (-1) \cdot \sum_{t=1}^{T} (Ggen_t \cdot PRsub_t \cdot TL), \\ \text{Ben} = (-1) \cdot \sum_{t=1}^{T} \{TL \cdot PRcoal \cdot Gb_t\}. \end{cases} \tag{7}$$

In Eq. 7, *PRsub* represents the price of government compensation. *PRcoal* represents the local price of electricity generated from desulfurized fire coal. Gb_t represents the PV generation power (kW) at the *t*th time step. Details of Gb_t are given in Equations 8 and (9).

$$Gb_t = Min - sele[(Ggen_t - Puse_t)| \cdot R_t, Ggen_t], \tag{8}$$

$$R_t = \frac{|\,Ggen_t - Puse_t\,| + (Ggen_t - Puse_t)}{2 \cdot (Ggen_t - Puse_t)}, \tag{9}$$

where the function *Min_sele( )* receives two scalar inputs and outputs the lower value. The reason for choosing the function *Min_sele* is that SFI only admits the power generated from the SFI PV panel to feed into the grid. If the feed-in power load is larger than $Ggen_t$, the extra section is not admitted. The ratio R_t gives the benefit from the consumer to the grid.

Turning to microgrid cost with high industrial implementation potential, the aim of the microgrid is to satisfy the operational requirements with a minimum cost for industrial and commercial consumers. The objective function of microgrid operation is given in Eq. 10.

$$F = C_{TOU} + C_{capicity} + C_{anci} + C_{PV}, \tag{10}$$

$$Min : Obj = F + \mu \cdot \sum_{j=1}^{J} \sigma_j. \tag{11}$$

It is assumed that there are J periods within 1 day. The dynamic daily electricity price in each period is the same. Then, σ_j in (11) represents the standard deviation of P_{load} in the *j*th period. Eq. 11 adds a regulation of fluctuation in the objective function to control the fluctuation degree.

Tariffs may not prevent all economic equivalence of all daily time periods. For example, the price value is the same under TOU for the same period. Even real-time prices may contain periods with similar price levels. In this period with similar economic equivalence, different response schemes with the same total consumption may have the same cost, leading to multiple optimal points of optimization. Some of these optimal points may contain high response fluctuation between different time periods that consumers find difficult to follow. A fluctuation regulation term is added to the objective function Eq. 11 to reject the solution with high fluctuation so that the potential for consumer implementation is increased.

3 Response of electric/thermal storage

3.1 Microgrid electrical network

Figure 1 introduces a typical electrical network of a large group of consumers.

Figure 1 shows a typical microgrid of a large group of consumers with the following devices: devices for manufacturing or other vocational devices, electricity storage, and distributed generation, including PV and electric-supported equipment in a cooling network. Eq. 12 gives the total power load from the electrical network.

$$\begin{cases} P_{load} = P_{other} + P_{cool} + P_{ES}^{chr}, \\ P_{cool} = \sum_{n=1}^{2} \left[P_{ch,n}(t) + P_{pump,n} \right] \cdot S_{w,n}(t), \end{cases} \tag{12}$$

$$S_{w,n}(t) = \begin{cases} 0, \text{switched off}, \\ 1, \text{switched on}, \end{cases} \tag{13}$$

where P_{other} represents the time series load vector of all devices except electricity storage and devices in the cooling system. The element $P_{ch,n}(t)$ represents the value of the *n*th chiller power at the *t*th time step. $P_{pump,n}$ represents the power of the *n*th pump. Due to the scheme of chiller control, the pumping power is usually kept at the same value. As this work studies storage response, P_{other} is set to be an unchangeable boundary condition during optimization. The pumping power is usually kept at a large constant value, which ensures a sufficient flow rate for the security of chiller operations. It will be changed when the pump and chiller are switched off together. Thus, $S_{w,n}(t)$ in Eq. 13 represents the on–off status of chiller n and is between 0 and 1.

3.1.1 Electricity storage response

Naturally, the operation of the electricity storage must be within its physical limit. The first limit is that the rate of charging or discharging should satisfy the storage's security. Eq. 14 introduces the limit as constraints. In Eq. 15, P_{ES}^{max} represents the maximum charging rate, and P_{ES}^{min} represents the maximum discharging rate (negative). Eq. 15 reflects the continuously adjusting capability of electricity storage performance.

$$P_{ES}^{min} \le P_{ES}(t) \le P_{ES}^{max}, \tag{14}$$

where $P_{ES}(t)$ represents the value of charging power at the tth time step.

The second limit is that the energy stored in electricity storage must be within its maximum and minimum limits. Eq. 15 shows this limit.

$$E_{ES}^{min} \le E_{ES}(t) \le E_{ES}^{max}, \tag{15}$$
$$E_{ES}(t) = E_{ES}(t-1) + TL \cdot P_{ES}(t),$$

where $E_{ES}(t)$ represents the value of stored energy at the tth time step.

If the consumer joins MRGPAS and has contracted with power plants at the specified time, the power of charging is fixed by the constraints detailed in the bid and contracts. Eq. 16 introduces this constraint.

$$P_{ES}(t) = P_{anci}(t), \text{if } H(t) = 1. \tag{16}$$
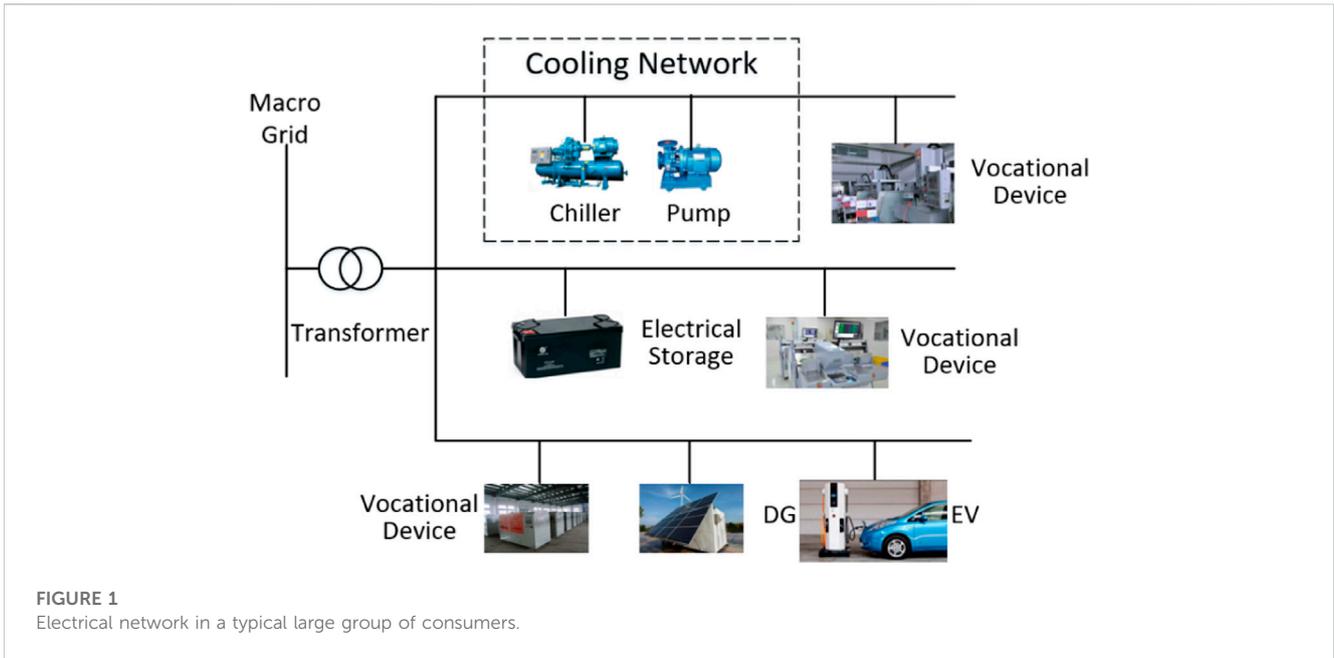
FIGURE 1
Electrical network in a typical large group of consumers.

TABLE 1 Relevant boundary conditions of the numerical study.

TOU in CP		Parameter	Value
0:00–8:00	0.3461 CNY/kWh	Pump power	30 kW
8:00–14:00	0.6473 CNY/kWh	P_{ES}^{min}	−10,000 kW
14:00–17:00	1.039 CNY/kWh	P_{ES}^{max}	10,000 kW
17:00–19:00	0.6473 CNY/kWh	E_{ES}^{min}	10,000 kWh
19:00–22:00	1.039 CNY/kWh	E_{ES}^{max}	50,000 kWh
22:00–24:00	0.6473 CNY/kWh	P_{ch}^{max}	40 kW
-	-	Q_{in}^{min}	−8,000 kW
-	-	Q_{in}^{max}	8,000 kW
-	-	$COhs^{min}$	3,200 kWh
-	-	$COhs^{max}$	25,500 kWh

3.2 Microgrid cooling network

A typical cooling network for a large group of consumers is shown in Figure 2.

The cooling network is for the generation and transmission of cold from chillers to consumers' space. From Figure 2, chiller units are the only cold generation system in the network. The cold generated will be passed to the user network to satisfy the cooling requirement or be stored in cold storage.

3.3 Dynamic transformation rate from electrical power to cooling power

Cold is initially generated by chillers in a cooling network. COP is widely preferred to evaluate a chiller's cold generation efficiency. Eq. 17 gives this relationship.

$$E_{CS,n}(t) = P_{ch,n}(t) \cdot COP_n(t), n = 1, 2 \tag{17}$$

COP is not a constant. It will change while P_{ch} changes. Figure 3 shows the operational statistics among COP, P_{ch}, and E_{CS}.

As shown in Figure 3, COP decreases nonlinearly while P_{ch} increases. Thus, there is a peak point of E_{CS} in the range of P_{ch}. With curve fitting, the approximation of COP and E_{CS} in Figure 3 is given by Eq. 20, which is the red line in the figure. The result of Eq. 18 is based on polynomial approximation.

$$E_{CS,i}(t) = \sum_{m=0}^{6} \alpha_m \cdot P_{ch,i,j}(t). \tag{18}$$

Moreover, the power of each chiller should not exceed its rated working range given in Eq. 19.

$$P_{ch}^{min} \leq P_{ch}(t) \leq P_{ch}^{max}. \tag{19}$$

On a certain day, the requirement of time series indoor temperature depends on the requirements of vocational work, so the time series cold requirement is constant. To balance the cold generation and consumption, the cooling network should satisfy the requirement given in Eq. 20.

$$\sum_{n=1}^{2} E_{CS,n}(t) \cdot S_{w,n}(t) = Q_{tot}(t) + Q_{in}(t), \tag{20}$$

where $Q_{tot}(t)$ represents the cold consuming rate of the microgrid at the tth time step. $Q_{in}(t)$ represents the cold charging rate of cold storage at the tth time step. Eq. 17 shows that the generated cold will be either consumed by the microgrid's cooling requirements or by charging the cold storage.

In Figure 2, the power exchanging speed of cold storage can be controlled by thermal energy exchanging areas through switching the corresponding valves, so the control of charging/discharging rate in cold storage can be given by Eq. 21. Q_{in}^{max} and Q_{in}^{min} represent the maximum and minimum charging rates of cold storage, respectively.
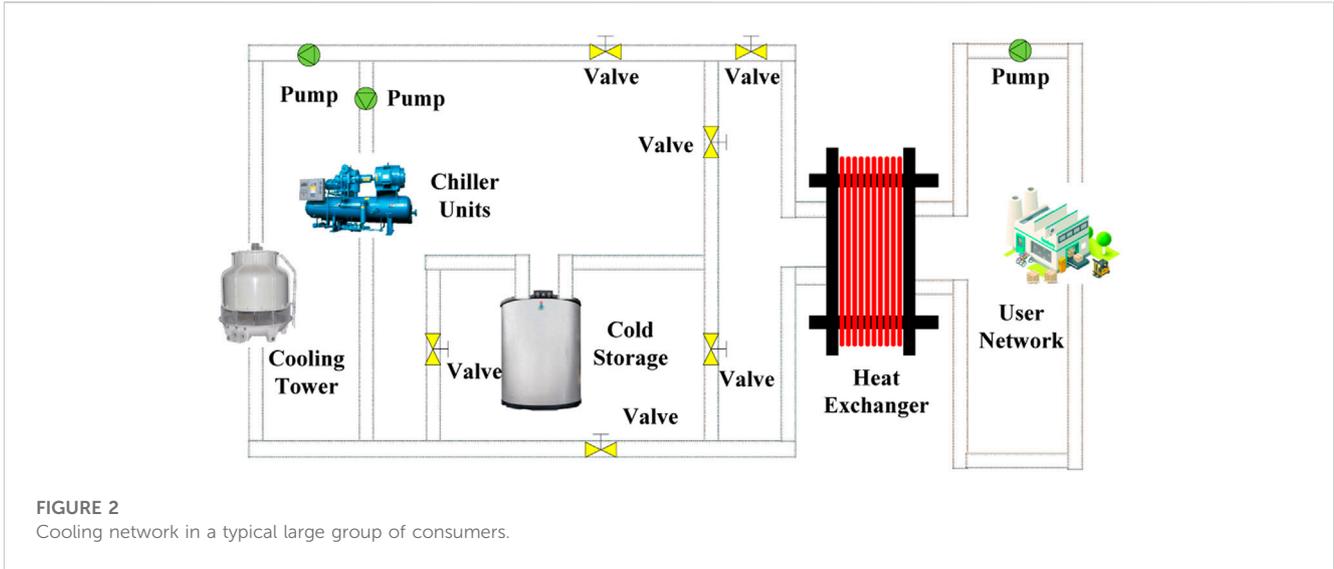
FIGURE 2
Cooling network in a typical large group of consumers.
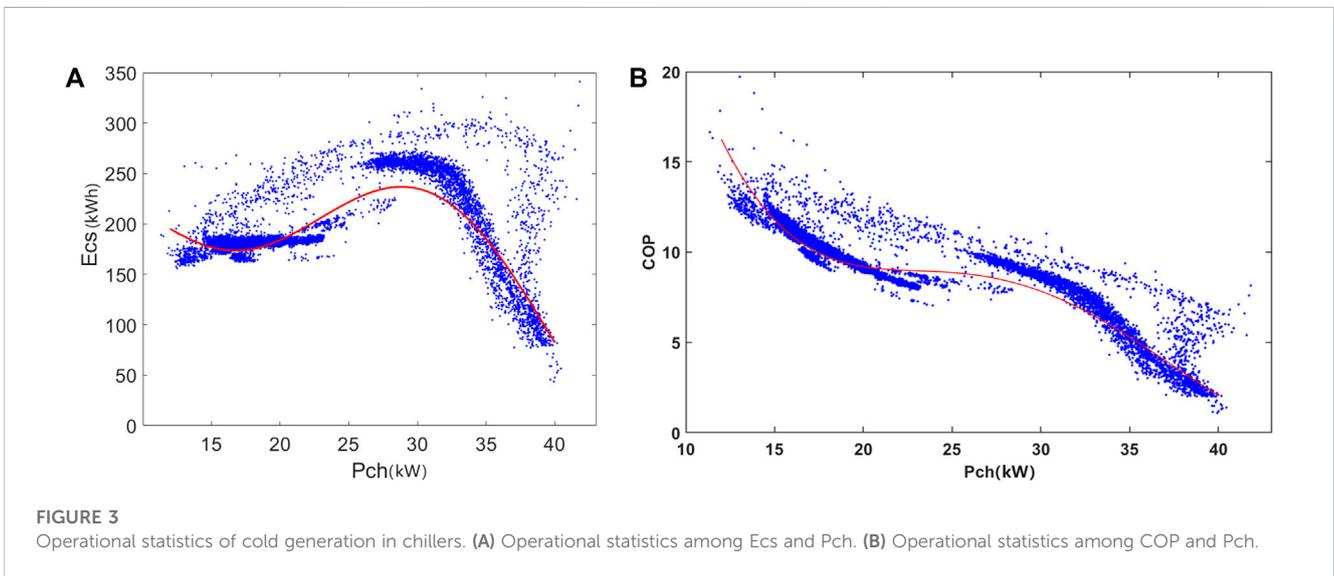
FIGURE 3
Operational statistics of cold generation in chillers. **(A)** Operational statistics among Ecs and Pch. **(B)** Operational statistics among COP and Pch.

$$Q_{in}^{\min} \le Q_{in}(t) \le Q_{in}^{\max}. \tag{21}$$

Eq. 22 gives the limits for cold storages, where $COhs_t$ represents the value of stored cold at the tth time step.

$$\begin{cases} COhs^{\min} \le COhs_t \le COhs^{\max} \\ COhs_t = Qin(t) \cdot TL + COhs_{t-1}. \end{cases} \tag{22}$$

Eq. 22 shows that cold storage cannot exceed its maximum and minimum operational limits at any time of the day.

For an electric vehicle charging station, the probability density function (PDF) of the arrival time of EVs is described by Eq. 23:

$$f_{EV}^{ar}(t) = \begin{cases} \dfrac{1}{\sqrt{2\pi}\sigma_1} \exp\left[-\dfrac{(t+24-\mu_1)^2}{2\sigma_1^2}\right] & 0 < t \le \mu_1 - 12, \\ \dfrac{1}{\sqrt{2\pi}\sigma_1} \exp\left[-\dfrac{(t-\mu_1)^2}{2\sigma_1^2}\right] & \mu_1 - 12 < t \le 24, \end{cases} \tag{23}$$

where μ and μ_1 are the mean values of the time when EVs arrive and depart from EVCS, respectively, and σ_1 and σ_2 are the standard deviations of the time when EVs arrive and leave EVCS, respectively.

The daily load demand of EV charging is related to the daily driving mileage and charging duration. In general, the daily travel mile of an EV is considered to obey a normal distribution, and its PDF is described by Eq. 24:

$$f_M(M_d) = \frac{1}{\sqrt{2\pi}\sigma_M M_d} \exp\left[-\frac{(\ln M_d - \mu_M)^2}{2\sigma_M^2}\right], \tag{24}$$

where M_d represents the daily mileage of EVs and σ_M and μ_M are the standard deviation and the mean value of M_d, respectively.

4 Numerical study and analysis

4.1 Material and methods

To analyze the storage impact under multiple market accesses and verify model feasibility, a numerical study with practical data is implemented. The device's power load time series under general operation is selected from a typical factory. The TOU tariff data used

FIGURE 4
Electric vehicle power consumption.

FIGURE 5
Optimization result of storage performance in case study 1. **(A)** Dynamic daily electricty Price **(B)** Daily total load **(C)** Electricity storage performance **(D)** Cold storage performance.
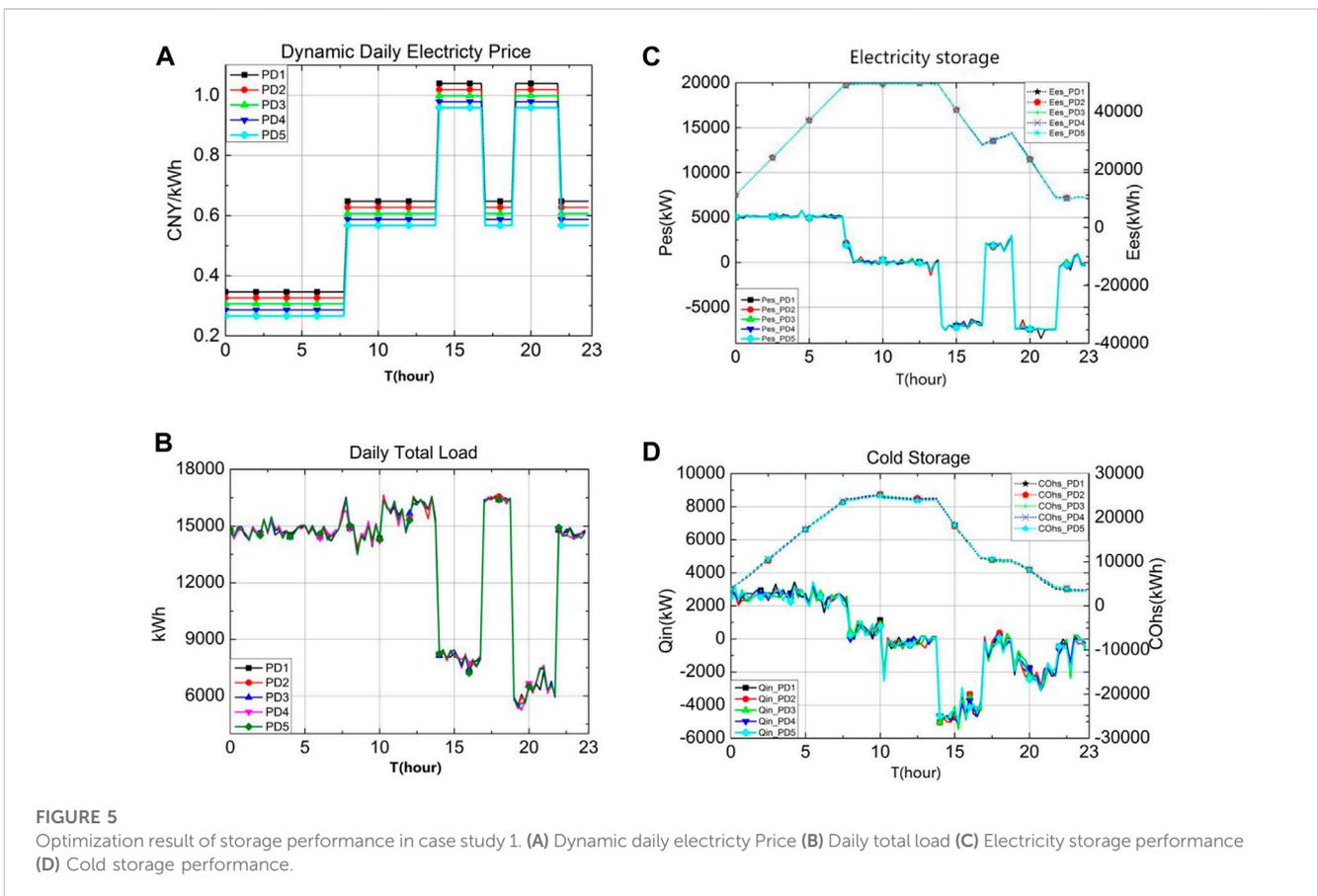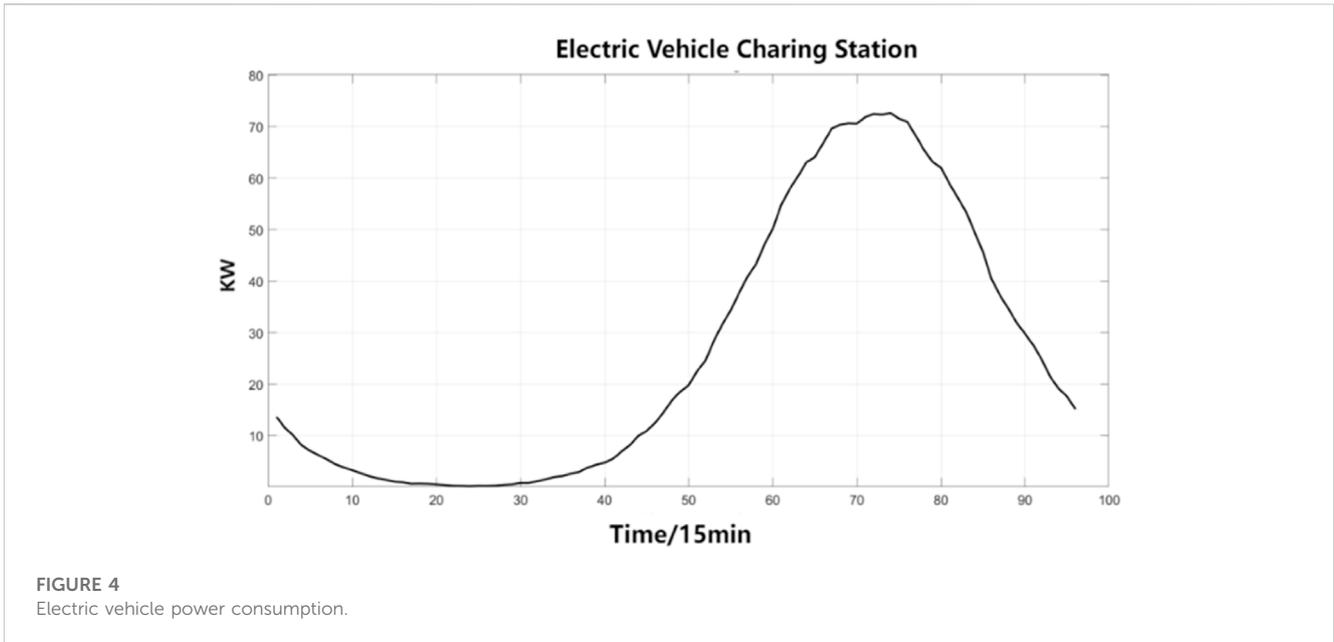
in this study were sourced from the official website of the Guangdong Provincial Development and Reform Commission in China. The compensation bid price of MRGPAS is assumed to be at its lowest limit, that is, 0.1 CNY/kWh. This assumption ensures the minimum benefit and the participation of the target factory in MRGPAS. MRGPAS

also provides a bottom limit for participating electricity storage's maximum charging/discharging rate, which is 10 MW.

The cooling system in this target factory contains three sub-cooling units. Each unit includes eight chillers connecting together on the same flowing pipe. Each chiller is associated with an

TABLE 2 Cost analysis under different MRGPAS participation time periods.

Scenario	Participation time	Cost from TOU (CNY)	Cost from CBC (CNY)	Cost from MRGPAS (CNY)	Total cost (CNY)
0	None	185,363.2	17,989.4	0.0	203,352.6
1	2:00–3:00	183,828.9	17,535.6	1,501.1	202,865.6
2	2:00–4:00	181,374.7	17,453.0	3,002.2	201,830.0
3	2:00–5:00	172,327.2	21,254.3	7,382.9	200,964.4
4	2:00–6:00	168,903.8	21,259.7	9,843.9	200,007.4
5	2:00–7:00	169,888.6	19,037.4	9,843.9	198,770.0

independent pump. The total cooling requirement is collected from a typical day in summer in the factory's historical data.

The target factory has one flywheel electric power storage group and one phase-changing cold power storage. The relevant boundary conditions in the numerical study are given in Table 1. As stochastic optimization is one of the typical methods for microgrid planning, the genetic algorithm is selected to solve the optimization. MATLAB GA Global Optimization Toolbox was used to carry out the study. The crossover rate was set at 0.8, while the mutation rate was at 0.01. The numerical study was carried out in MATLAB (version R2019a) on a computer with an AMD Ryzen 71,700 Eight-Core Processor, 3.00 GHz, and 8.0 GB of RAM.

4.2 Case 1: storage performance on binary market accesses: TOU with price difference and capacity-based charging

Case study 1 aims to demonstrate the storage performance when the microgrid joins dynamic daily electricity price and CBC together. Figures 5A–D show the optimization results.

From Figures 5A–D, the following three main points are observed:

Dynamic daily electricity price promotes storages to charge when the price is low and discharge when the price is high. The energy stored in both storages increases when the price is low and decreases when the price is high. The reason for this is that the cost of the microgrid will be decreased by consuming cheaper energy.

Different PD values will not influence the storage performance. As shown in Figure 4, results under different PD values are nearly the same. The reason for this is that the optimal cost of the microgrid under TOU only depends on the shape of the price curve. Because the same PD is added to the price level at each hour, shifting the price curve entirely will not change the relationship of price between any two time points. Therefore, time with a lower price will always be lower in different PD values, and different PD values will not influence the cost from CBC. Thus, catalog price with PD will not influence the storage performance.

The discharging rate of energy storage systems does not reach its maximum in price-peak time. Figure 4 shows that the absolute value of the discharging rate is still smaller than the storage's maximum discharging rate. There is a remaining
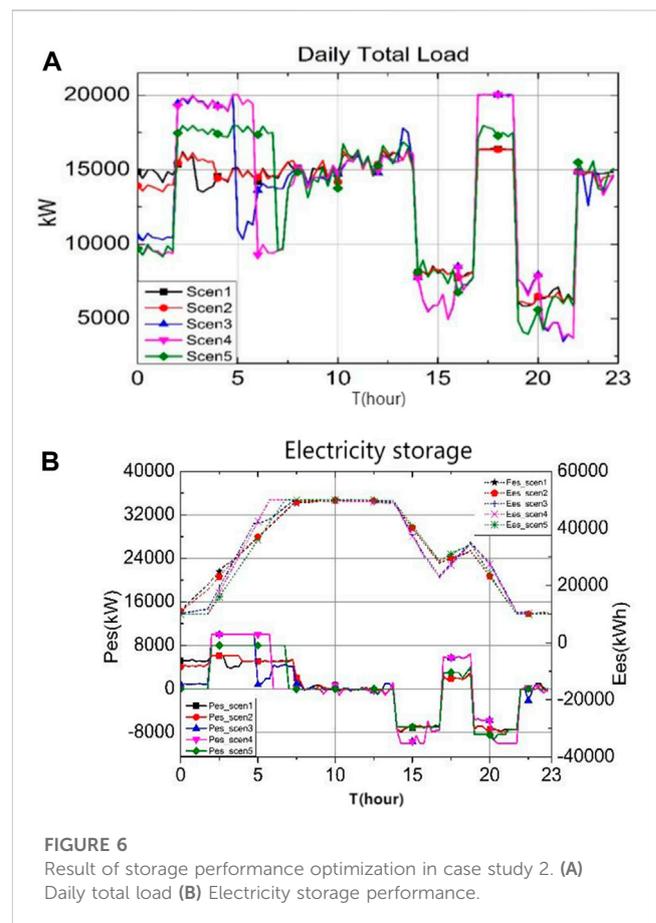
FIGURE 6
Result of storage performance optimization in case study 2. **(A)** Daily total load **(B)** Electricity storage performance.

discharging capability in price-peak time. The reason for this is that the marginal cost from CBC will increase faster than cost reduction under TOU if the discharging rate increases in price-peak time.

4.3 Case 2: storage behavior in three-traffic market accesses: TOU with price difference, CBC, and MRGPAS

Case study 2 demonstrates the storage performance when the microgrid is under three-market accesses together. Considering that MRGPAS has a focus on renewable power generation, the bid of MRGPAS is assumed to happen at nighttime, for most wind
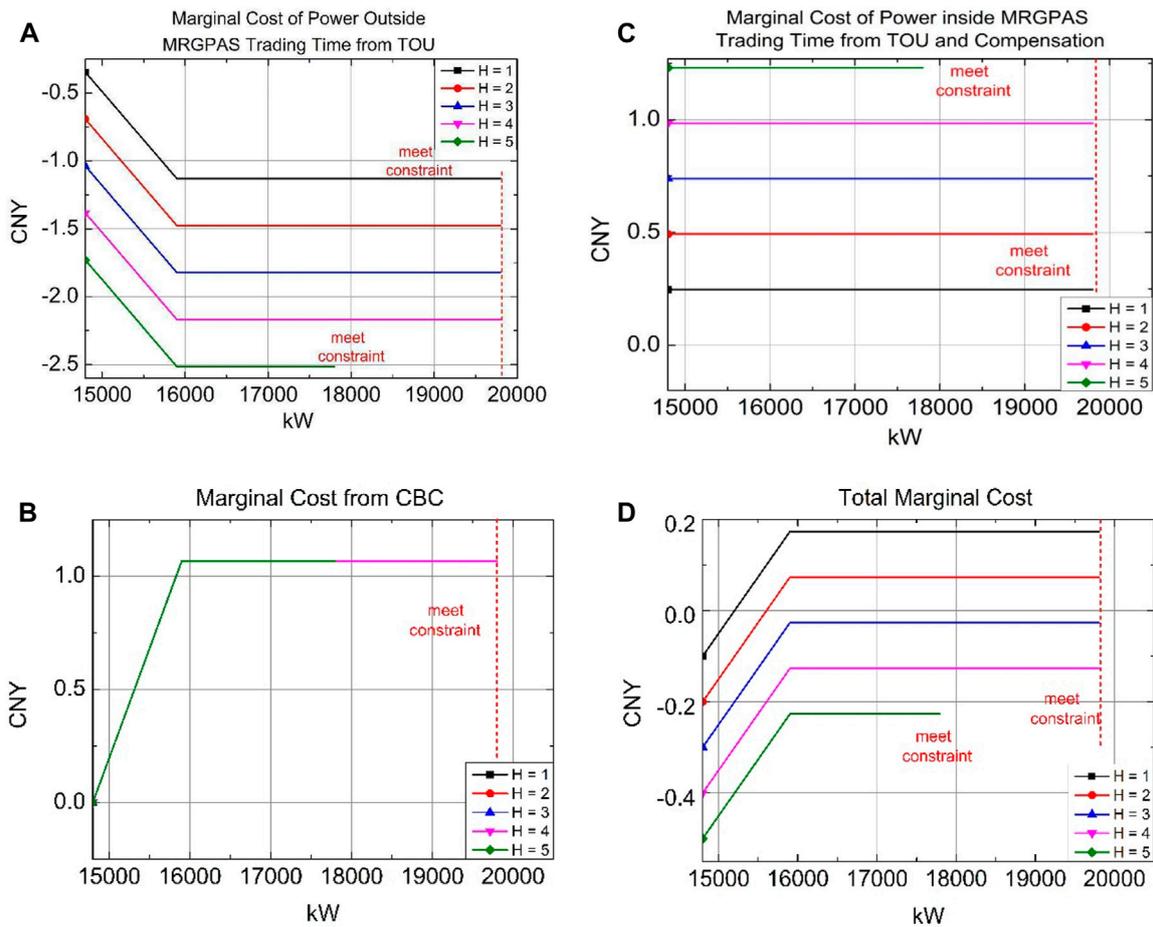
FIGURE 7
Marginal cost variation under three-market accesses. **(A)** Marginal cost of Powepr outside MRGPAS trading time from TOU. **(B)** Marginal cost from CBC. **(C)** Marginal cost of power inside MRGPAS trading time from TOU and compensation. **(D)** Total marginal cost.

FIGURE 8
Cost variation details under three-market accesses.

FIGURE 9
Microgrid operation under four-market accesses. **(A)** Daily total load and generated power. **(B)** Response behavior of electrical storage.

TABLE 3 Microgrid cost analysis under four-market accesses.

Market accesses	Without PV	With PV
Cost from TOU (CNY/kWh)	169,888.60	164,405.05
Cost from CBC (CNY/kWh)	19,037.42	18,988.87
Cost from MRGPAS (CNY/kWh)	9,843.93	9,843.91
Cost from solar generation (CNY/kWh)	0	−3,955.92
Total cost (CNY/kWh)	198,769.95	189,281.91

In addition, the load in the target period is limited to a threshold in case study 1 when the marginal cost of CBC becomes positive. Therefore, when charging power inside the MRGPAS trading time increases at night, the threshold of load limitation in the target period could be increased. Thus, the remaining capability in price-peak time can be shifted to the time between 17:00 and 19:00, which can reduce the cost further. When MRGPAS trading is larger than or equal to 3 h, the sum of MRGPAS compensation and threshold releasing will be larger than the cost increase of CBC. Thus, more charging power can be added inside the MRGPAS trading time. Reflecting on Figure 7 d), the marginal cost of H≥3 is negative, and so the cost will be decreased.

Figure 8 show the comparison of optimal cost under different trading time lengths. It shows that increasing the time length of the MRGPAS trading time will decrease the microgrid's cost. Analysis of this case study shows that the time length of the MRGPAS bid will influence the cost in all three markets and thus influence the storage performance.

4.4 Case 3: storage performance in four-market accesses

When the microgrid is integrated with distributed solar generation, less power from the grid is needed. This case study integrates all four-market accesses together for microgrid analysis. A typical daily generation capacity variation is shown in Figures 9A, B. Figures 9A, B and Table 3 give the results of solar generation. Scenario 5 from case study 3 is selected for MRGPAS access in this case study.

From Figures 9A, B, solar generation integration in a large network of consumers will compensate for an obvious section of the power consumption between 8:00 and 19:00. Between 14:00 and 17:00, the price reaches the maximum level in TOU; therefore, storages and PV panels will output their electricity to decrease the total load. Finally, the cost from TOU will be reduced from 169,888 CNY/day to 164,405 CNY/day for solar generation, and the microgrid will receive approximately 4,000 CNY/day as governmental compensation. Generally, solar power generation mainly occurs in the daytime. Thus, it only duplicates with the discharging of storage. The CBC reference and MRGPAS do not occur within these areas, and thus, solar power generation will not influence the response behavior of storage.

generation abandonment occurs at night. Figures 5A–D and Table 2 give the result of optimization on different time lengths of MRGPAS participation. From MRGPAS requirements, cold storage is not allowed to join MRGPAS.

From Figures 6A, B, the following two points can be seen.

At the time of MRGPAS trading, the charging rate of electrical storage is higher than the charging rate outside of MRGPAS trading time at night. The reason for this is that charging within the MRGPAS bid will generate extra revenue from the MRGPAS market other than charging under the daily dynamic price tariff. Therefore, a greater amount of charging rate is shifted into MRGPAS trading time in all scenarios. This means that choosing to release the control of electricity storage to charge in MRGPAS trading will lead to a lower cost than charging under the daily dynamic price.

The charging rate of electric storage will rise to a higher level than the charging rate outside the MRGPAS trading time at night when the length of trading time is not less than 3 h. When the length of trading time is larger than or equal to 3 h, the charging rate within trading time will have a significant increase. This phenomenon is due to the comparison between the marginal cost in CBC and that of MRGPAS trading. A detailed analysis is given in Figures 7A–D.

Due to the compensation from the MRGPAS market, power shifts from outside the MRGPAS trading time to the trading time, which can generate extra benefits from MRGPAS. This shifting will increase the reference power and cost of CBC.

5 Conclusion

This paper presents market models with four different types of tariffs for the microgrid market environment. The performance of both electricity storage and cold storage systems is modeled to formulate a non-linear mixed-integer programming problem. The numerical study shows that different market accesses will influence the storage system's response together. A trade-off of different market participation occurs on storage performance. However, generally, a microgrid with energy storage systems will achieve a reduced cost with more market participation. From the study and discussion, a better insight was provided into energy trading within a microgrid, including energy storage. A future work based on standard development could be considered.

Data availability statement

The raw data supporting the conclusions of this article will be made available by the authors, without undue reservation.

Author contributions

MY: conceptualization, data curation, investigation, methodology, writing–original draft, and writing–review and editing. ZL: conceptualization, formal analysis, investigation, methodology, and writing–original draft. CL: conceptualization, formal analysis, investigation, resources, and writing–review and editing. ZZ: conceptualization and writing–review and editing. AZ: writing–review and editing. LL: funding acquisition, methodology, resources, supervision, writing–original draft, and writing–review

and editing. ZS: data curation, formal analysis, project administration, and writing–review and editing.

Funding

Conflict of interest

Author MY was employed by Jiangmen Power Supply Bureau of Guangdong Power Grid Co Ltd. Author ZS was employed by China Southern Power Grid Co. Ltd.

The remaining authors declare that the research was conducted in the absence of any commercial or financial relationships that could be construed as a potential conflict of interest.

The author(s) declared that they were an editorial board member of Frontiers, at the time of submission. This had no impact on the peer review process and the final decision.

Publisher's note

References

Al-Awami, A. T., Amleh, N. A., and Muqbel, A. M. (2017). Optimal demand response bidding and pricing mechanism with fuzzy optimization: application for a virtual power plant. *IEEE Trans. Industry Appl.* 53 (5), 5051–5061. doi:10.1109/tia.2017.2723338

Amrollahi, M. H., and Bathaee, S. M. T. (2017). Techno-economic optimization of hybrid photovoltaic/wind generation together with energy storage system in a stand-alone micro-grid subjected to demand response. *Appl. energy* 202, 66–77. doi:10.1016/j.apenergy.2017.05.116

Chen, T. H., Hsieh, T. Y., Yang, N. C., Yang, J. S., and Liao, C. J. (2013). Evaluation of advantages of an energy storage system using recycled EV batteries. *Int. J. Electr. Power & Energy Syst.* 45 (1), 264–270. doi:10.1016/j.ijepes.2012.08.037

Chen, W., Qiu, J., Zhao, J., Chai, Q., and Dong, Z. Y. (2021). Bargaining game-based profit allocation of virtual power plant in frequency regulation market considering battery cycle life. *IEEE Trans. Smart Grid* 12 (4), 2913–2928. doi:10.1109/tsg.2021.3053000

Fan, W., Huang, L. L., Cong, B., Degejirifu, Tan, Z., and Xing, T. (2022). Research on an optimization model for wind power and thermal power participating in two-level power market transactions. *Int. J. Electr. power & energy Syst.* 134, 107423. doi:10.1016/j.ijepes.2021.107423

Garcia-Torres, F., Bordons, C., Tobajas, J., Marquez, J. J., Garrido-Zafra, J., and Moreno-Munoz, A. (2020). Optimal schedule for networked microgrids under deregulated power market environment using model predictive control. *IEEE Trans. Smart Grid* 12 (1), 182–191. doi:10.1109/tsg.2020.3018023

Gough, R., Dickerson, C., Rowley, P., and Walsh, C. (2017). Vehicle-to-grid feasibility: a techno-economic analysis of EV-based energy storage. *Appl. energy* 192, 12–23. doi:10.1016/j.apenergy.2017.01.102

Hakimi, S. M., and Moghaddas-Tafreshi, S. M. (2014a). Optimal planning of a smart microgrid including demand response and intermittent renewable energy

resources. *IEEE Trans. Smart Grid* 5 (6), 2889–2900. doi:10.1109/tsg.2014.2320962

Hakimi, S. M., and Moghaddas-Tafreshi, S. M. (2014b). Optimal planning of a smart microgrid including demand response and intermittent renewable energy resources. *IEEE Trans. Smart Grid* 5 (6), 2889–2900. doi:10.1109/tsg.2014.2320962

He, G., Chen, Q., Kang, C., Xia, Q., and Poolla, K. (2016). Cooperation of wind power and battery storage to provide frequency regulation in power markets. *IEEE Trans. Power Syst.* 32 (5), 3559–3568. doi:10.1109/tpwrs.2016.2644642

Huang, H., Nie, S., Lin, J., Wang, Y., and Dong, J. (2020). Optimization of peer-to-peer power trading in a microgrid with distributed PV and battery energy storage systems. *Sustainability* 12 (3), 923. doi:10.3390/su12030923

Jiang, Z., Hlanze, P., and Cai, J. (2022). Optimal predictive control of phase change material-based energy storage in buildings via mixed-integer convex programming. *Appl. Therm. Eng.* 215, 118821. doi:10.1016/j.applthermaleng.2022.118821

Khalilpour, K. R., and Vassallo, A. (2016). A generic framework for distributed multi-generation and multi-storage energy systems. *Energy* 114, 798–813. doi:10.1016/j.energy.2016.08.029

Khaloie, H., Toubeau, J. F., Vallée, F., Lai, C. S., and Lai, L. L. (2021). An innovative coalitional trading model for a biomass power plant paired with green energy resources. *IEEE Trans. Sustain. Energy* 13 (2), 892–904. doi:10.1109/tste.2021.3138777

Kumar, G. V. B., and Palanisamy, K. (2020). A review of energy storage participation for ancillary services in a microgrid environment. *Inventions* 5 (4), 63. doi:10.3390/inventions5040063

Kwon, S., Ntaimo, L., and Gautam, N. (2016). Optimal day-ahead power procurement with renewable energy and demand response. *IEEE Trans. Power Syst.* 32 (5), 3924–3933. doi:10.1109/tpwrs.2016.2643624

Lai, C. S., Jia, Y., Lai, L. L., Xu, Z., McCulloch, M. D., and Wong, K. P. (2017b). A comprehensive review on large-scale photovoltaic system with applications of electrical energy storage. *Renew. Sustain. Energy Rev.* 78, 439–451. doi:10.1016/j.rser.2017.04.078

Lai, C. S., Jia, Y., McCulloch, M. D., and Xu, Z. (2017a). Daily clearness index profiles cluster analysis for photovoltaic system. *IEEE Trans. Industrial Inf.* 13 (5), 2322–2332. doi:10.1109/tii.2017.2683519

Lai, C. S., Jia, Y., Xu, Z., Lai, L. L., Li, X., Cao, J., et al. (2017c). Levelized cost of electricity for photovoltaic/biogas power plant hybrid system with electrical energy storage degradation costs. *Energy Convers. Manag.* 153, 34–47. doi:10.1016/j.enconman.2017.09.076

Lai, C. S., and McCulloch, M. D. (2016). Sizing of stand-alone solar PV and storage system with anaerobic digestion biogas power plants. *IEEE Trans. Industrial Electron.* 64 (3), 2112–2121. doi:10.1109/tie.2016.2625781

Lai, C. S., and McCulloch, M. D. (2017). Levelized cost of electricity for solar photovoltaic and electrical energy storage. *Appl. energy* 190, 191–203. doi:10.1016/j.apenergy.2016.12.153

Li, X., Wang, L., Yan, N., and Ma, R. (2021). Cooperative dispatch of distributed energy storage in distribution network with PV generation systems. *IEEE Trans. Appl. Supercond.* 31 (8), 1–4. doi:10.1109/tasc.2021.3117750

Lin, J., Kahrl, F., Yuan, J., Liu, X., and Zhang, W. (2019). Challenges and strategies for electricity market transition in China. *Energy Policy* 133, 110899. doi:10.1016/j.enpol.2019.110899

Liu, Z., Chen, Y., Zhuo, R., and Jia, H. (2018). Energy storage capacity optimization for autonomy microgrid considering CHP and EV scheduling. *Appl. Energy* 210, 1113–1125. doi:10.1016/j.apenergy.2017.07.002

MansourLakouraj, M., Shahabi, M., Shafie-khah, M., and Catalão, J. P. (2022). Optimal market-based operation of microgrid with the integration of wind turbines, energy storage system and demand response resources. *Energy* 239, 122156. doi:10.1016/j.energy.2021.122156

Olabi, A. G. (2017). Renewable energy and energy storage systems. *Energy* 136, 1–6. doi:10.1016/j.energy.2017.07.054

Rabiee, A., Farahani, H. F., Khalili, M., Aghaei, J., and Muttaqi, K. M. (2016). Integration of plug-in electric vehicles into microgrids as energy and reactive power providers in market environment. *IEEE Trans. Industrial Inf.* 12 (4), 1312–1320. doi:10.1109/tii.2016.2569438

Rostamnezhad, Z., Mary, N., Dessaint, L. A., and Monfet, D. (2022). Electricity consumption optimization using thermal and battery energy storage systems in buildings. *IEEE Trans. Smart Grid* 14 (1), 251–265. doi:10.1109/tsg.2022.3194815

Tabar, V. S., Ghassemzadeh, S., and Tohidi, S. (2019). Energy management in hybrid microgrid with considering multiple power market and real time demand response. *Energy* 174, 10–23. doi:10.1016/j.energy.2019.01.136

Tian, X., Chen, W., and Hu, J. (2023). Game-theoretic modeling of power supply chain coordination under demand variation in China: a case study of Guangdong Province. *Energy* 262, 125440. doi:10.1016/j.energy.2022.125440

Valinejad, J., Marzband, M., Korkali, M., Xu, Y., and Saad Al-Sumaiti, A. (2020). Coalition formation of microgrids with distributed energy resources and energy storage in energy market. *J. Mod. Power Syst. Clean Energy* 8 (5), 906–918. doi:10.35833/mpce.2019.000116

Wang, C., Zhang, Z., Abedinia, O., and Farkoush, S. G. (2021). Modeling and analysis of a microgrid considering the uncertainty in renewable energy resources, energy storage systems and demand management in electrical retail market. *J. Energy Storage* 33, 102111. doi:10.1016/j.est.2020.102111

Xu, Z., Guan, X., Jia, Q. S., Wu, J., Wang, D., and Chen, S. (2012). Performance analysis and comparison on energy storage devices for smart building energy management. *IEEE Trans. Smart Grid* 3 (4), 2136–2147. doi:10.1109/tsg.2012.2218836

Zhang, T., Qiu, W., Zhang, Z., Lin, Z., Ding, Y., Wang, Y., et al. (2023). Optimal bidding strategy and profit allocation method for shared energy storage-assisted VPP in joint energy and regulation markets. *Appl. Energy* 329, 120158. doi:10.1016/j.apenergy.2022.120158

Zhang, X., Chen, H., Xu, Y., Li, W., He, F., Guo, H., et al. (2017a). Distributed generation with energy storage systems: a case study. *Appl. Energy* 204, 1251–1263. doi:10.1016/j.apenergy.2017.05.063

Zhang, X., Hug, G., Kolter, J. Z., and Harjunkoski, I. (2017b). Demand response of ancillary service from industrial loads coordinated with energy storage. *IEEE Trans. Power Syst.* 33 (1), 951–961. doi:10.1109/tpwrs.2017.2704524

Zhao, H., Hong, M., Lin, W., and Loparo, K. A. (2017). Voltage and frequency regulation of microgrid with battery energy storage systems. *IEEE Trans. smart grid* 10 (1), 414–424. doi:10.1109/tsg.2017.2741660

Zhao, T., and Ding, Z. (2017). Cooperative optimal control of battery energy storage system under wind uncertainties in a microgrid. *IEEE Trans. Power Syst.* 33 (2), 2292–2300. doi:10.1109/tpwrs.2017.2741672

Zhao, X., Lyon, T. P., and Song, C. (2012). Lurching towards markets for power: China's electricity policy 1985–2007. *Appl. energy* 94, 148–155. doi:10.1016/j.apenergy.2012.01.035

Zhao, Z., Xu, J., Guo, J., Ni, Q., Chen, B., and Lai, L. L. (2023). Robust energy management for multi-microgrids based on distributed dynamic tube model predictive control. *IEEE Trans. Smart Grid*, 1. (Early Access). doi:10.1109/tsg.2023.3290191

Zidan, A., Gabbar, H. A., and Eldessouky, A. (2015). Optimal planning of combined heat and power systems within microgrids. *Energy* 93, 235–244. doi:10.1016/j.energy.2015.09.039